Tropospheric Products from High-Level GNSS Processing in Latin America

María V. Mackern, María L. Mateo, María F. Camisay, and Paola V. Morichetti

Abstract

The present geodetic reference frame in Latin America and the Caribbean is given by a network of about 400 continuously operating GNSS stations. These stations are routinely processed by ten Analysis Centres following the guidelines and standards set up by the International Earth Rotation and Reference Systems Service (IERS) and International GNSS Service (IGS). The Analysis Centres estimate daily and weekly station positions and station zenith tropospheric path delays (ZTD) with an hourly sampling rate. This contribution presents some attempts aiming at combining the individual ZTD estimations to generate consistent troposphere solutions over the entire region and to provide reliable time series of troposphere parameters, to be used as a reference. The study covers ZTD and IWV series for a time-span of 5 years (2014–2018). In addition to the combination of the individual solutions, some advances based on the precise point positioning technique using BNC software (BKG NTRIP Client) and Bernese GNSS Software V.5.2 are presented. Results are validated using the IGS ZTD products and radiosonde IWV data. The agreement was evaluated in terms of mean bias and rms of the ZTD differences w.r.t IGS products (mean bias −1.5 mm and mean rms 6.8 mm) and w.r.t ZTD from radiosonde data (mean bias −2 mm and mean rms 7.5 mm). IWV differences w.r.t radiosonde IWV data (mean bias 0.41 kg/m^2 and mean rms 3.5 kg/m^2).

Keywords

IWV · Radiosonde · SIRGAS · ZTD

1 Introduction

Integrated Water Vapour (IWV) plays a fundamental role in several weather processes that deeply influence human activities. Retrieving IWV content in the atmosphere can be performed in different ways using independent techniques: from the traditional ones like radiosondes and ground-based microwave radiometers, up to the recent ones based on satellite techniques. In particular, the GNSS-based tropospheric Zenith Total Delay (ZTD) estimates allow inferring IWV values with high accuracy equivalent to that expected from

M. V. Mackern
Consejo Nacional de Investigaciones Científicas y Tecnológicas, Mendoza, Argentina

Facultad de Ingeniería. Universidad Nacional de Cuyo, Mendoza, Argentina

Facultad de Ingeniería. Universidad Juan Agustín Maza, Mendoza, Argentina
e-mail: vmackern@mendoza-conicet.gob.ar

M. L. Mateo (✉) · M. F. Camisay
Facultad de Ingeniería. Universidad Nacional de Cuyo, Mendoza, Argentina

Facultad de Ingeniería. Universidad Juan Agustín Maza, Mendoza, Argentina
e-mail: laura.mateo@ingenieria.uncuyo.edu.ar

P. V. Morichetti
Facultad de Ingeniería. Universidad Juan Agustín Maza, Mendoza, Argentina

International Association of Geodesy Symposia,
https://doi.org/10.1007/1345_2020_121,

direct observational techniques, such as radiosondes and microwave radiometers (Bonafoni et al. 2013; Van Baelen et al. 2005; Calori et al. 2016). Several studies have been devoted to the use of GNSS stations for the estimation of IWV over South America. Bianchi et al. (2016) estimated mean IWV based on GNSS data (IWV_{GNSS}) and its trends during 2007–2013 over more than a hundred GNSS tracking sites from SIRGAS-CON. Calori et al. (2016) analysed a period of 45 days where deep convective processes with hail precipitation took place over Mendoza province, in the Central-Western Argentina (CWA). For this assessment, the authors used IWV_{GNSS} maps to draw insight into the accumulation and influence of humidity over the region. Even fewer studies have performed a validation of the IWV_{GNSS}; for this, Fernández et al. (2010) used radiosonde data from four locations over Central-North Argentina in order to validate IWV estimates from Global Positioning System (GPS) stations during a 1-year period (2006–2007). The authors found an agreement between IWV_{GNSS} and IWV estimated through radiosonde data (IWV_{RS}), with differences as large as 3 kg/m^2. Llamedo et al. (2017) used GPS-derived IWV to analyse moisture anomalies over South America during El Niño-Southern Oscillation phases, finding positive anomalies over northern Argentina during El Niño events.

Camisay et al. (2020) estimated IWV_{GNSS} time series for a 4-year period (2015–2018), to assess the accuracy through a comparison in two GNSS Argentinean stations with radiosonde observations and explore the role of IWV in the development of regional precipitation events over the CWA. The obtained agreement between IWV_{GPS} and IWV_{RS} was close to 2 kg/m^2 in terms of mean absolute error. In Latin-American region, in situ meteorological observations are scarce; therefore, GNSS atmospheric monitoring has significant relevance for the understanding of regional meteorological processes. This kind of information is extremely valuable, and it can be used to achieve a better knowledge of IWV variable in the study region.

The GNSS allows monitoring the IWV from a network that surpasses traditional techniques due to its significant temporal and spacial density. This is of interest to study the regional trends of the climatic variable for which it is necessary to have a long time series by site and region. On the other hand, the ZTD can be estimated in real-time and near real-time mode, in order to be assimilated in regional forecast models.

SIRGAS (Sistema de Referencia Geocéntrico para las Américas) is the geocentric reference frame in Latin America and the Caribbean. It is at present given by a network of about 420 continuously operating GNSS stations (Cioce et al. 2018) (Fig. 1). These stations are routinely processed by the SIRGAS Analysis Centres (AC), following the guidelines and standards set up by the International Earth Rotation and Reference Systems Service (IERS) and International GNSS Service (IGS). Since 2014, the routine GNSS data processing includes the estimation of hourly ZTD values based on GPS and GLONASS observations (Camisay et al. 2020; Sánchez et al. 2015; Brunini et al. 2012).

Pacione et al. (2017) shows the great potential that a continental GNSS network offers in atmospheric studies. EUREF Permanent Network (EPN) (Bruyninx et al. 2019) had been used as a valuable database for the development of a climate data record of GNSS tropospheric products over Europe. It had been used as a reference in the regional numerical weather prediction reanalyses and climate model simulations and had been used for monitoring IWV trends and variability. Guerova et al. (2016) showed and discussed the advantages of the application of GNSS tropospheric products in operational weather prediction and in the climate monitoring.

In this contribution, we report on the estimation and validation of the ZTD and IWV values in Latin America GNSS stations, using as input data the ZTD values obtained in: (1) the operational processing of the SIRGAS regional reference frame and (2) applying the Precise Point Positioning (PPP) approach, with two softwares, BKG NTRIP Client (BNC) and Bernese v5.2. (BSW52). To assess the reliability of our results (ZTD and IWV values), they are compared with the operational IGS products (ZTD_{IGS}), IWV values extracted from radiosonde profiles (IWV_{RS}) and ZTD estimations inferred from integrate the correspondent radiosonde profile data (ZTD_{RS}).

In Sect. 2, the methodology used in operational SIRGAS processing to estimate ZTD product is reviewed. ZTD_{SIR} internal consistency is presented. ZTD products estimated by PPP in SIRGAS stations are reviewed. Section 3 summarises the ZTD_{SIR} and IWV_{SIR} products validation with respect to ZTD_{IGS} products and IWV radiosonde data. Conclusions, outlook and future work are given in Sect. 4.

2 Methodology

2.1 Estimation of ZTD Values Based on the Operational SIRGAS Processing (ZTD_{SIR})

The ZTD estimations based on the operational SIRGAS GNSS processing (ZTD_{SIR}) are routinely calculated for all the SIRGAS-CON stations (Fig. 1) by the SIRGAS Analysis

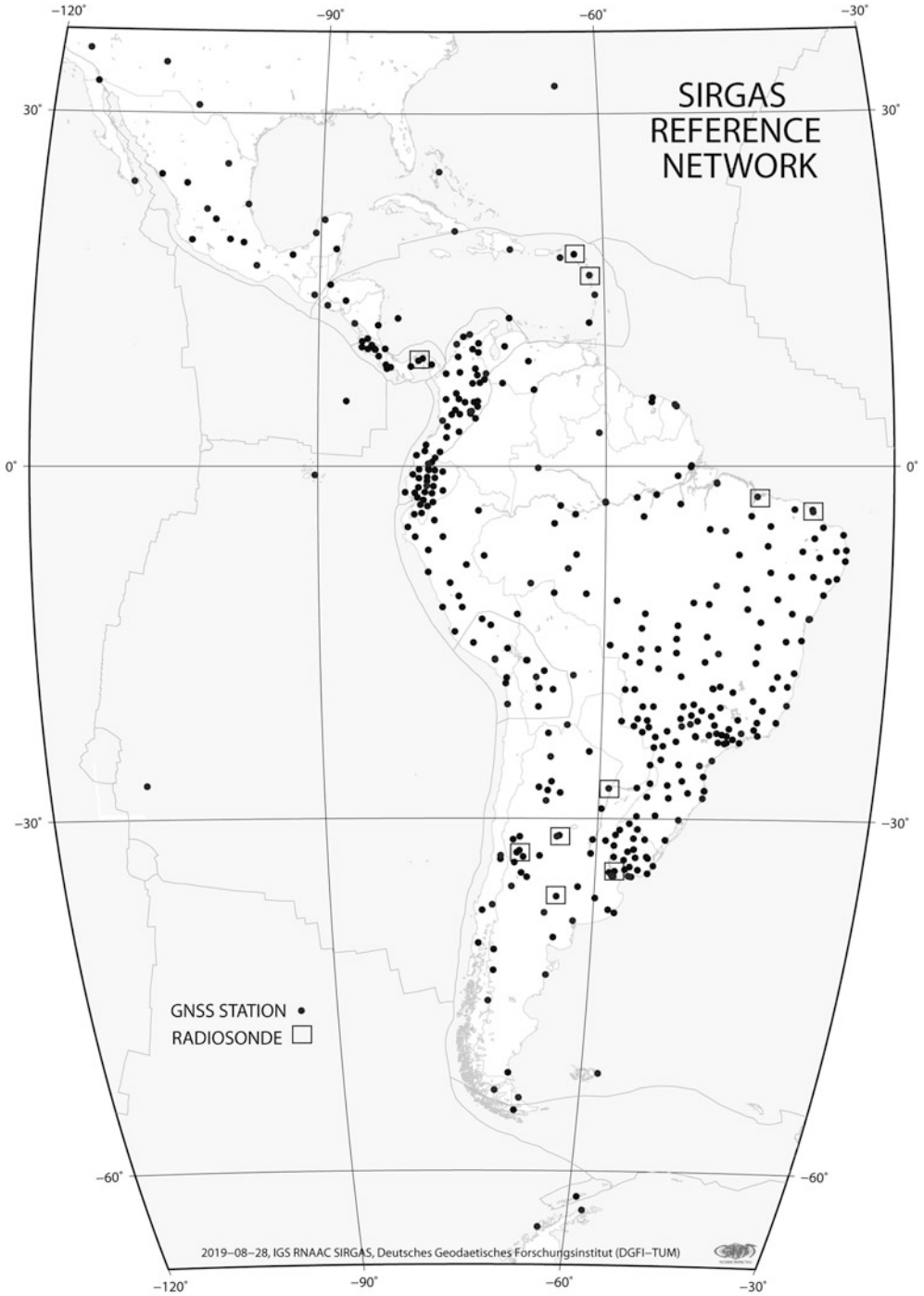

Fig. 1 SIRGAS GNSS stations and radiosonde sites considered in this study

Centres (AC) for a 5-year period (2014–2018). The eight official SIRGAS-AC (Table 1) used Bernese GNSS Software v5.2 (BSW52, Dach et al. 2015).

The SIRGAS operational ZTD products (ZTD_{SIR}) are calculated with the final IGS products (orbits and earth rotation parameters, ERP). Table 2 summarizes the methodology implemented for the operational SIRGAS products and the testing PPP products.

Each SIRGAS-AC processes a different sub-network of SIRGAS GNSS stations. The distribution of the stations considers that each station parameter (ZTD_i) is available in three different solutions, so it is possible to evaluate the

Table 1 SIRGAS Analysis Centres (AC) that estimated ZTD for the period 2014–2018

SIRGAS AC	Country	Institution	Software used	Start	End
DGF	Germany	Deutsches Geodätisches Forschungsinstitut der Technischen Universität München	BSW52	27 Apr. 2014	–
ECU	Ecuador	Instituto Geográfico Militar	BSW52	21 Dec. 2014	–
IBG	Brasil	Instituto Brasileiro de Geografia e Estatistica	BSW52	27 Apr. 2014	–
IGA	Colombia	Instituto Geográfico Agustín Codazzi	BSW52	21 Dec. 2014	–
CHL	Chile	Instituto Geográfico Militar	BSW52	27 Apr. 2014	–
URY	Uruguay	Instituto Geográfico Militar	BSW52	27 Apr. 2014	–
LUZ	Venezuela	Universidad de Zulia	BSW52	14 Dec. 2014	9 Feb. 2019
UNA	Costa Rica	Universidad Nacional de Costa Rica	BSW52	1 Jan. 2014	29 Dec.2018

Table 2 Models used for the ZTD estimation for the operational SIRGAS products and the testing PPP products

	Operational SIRGAS processing		Precise Point Positioning (PPP)	
Software	BSW52		BNC	BSW52
Observations	GPS + GLONASS		GPS + GLONASS	GPS
Sampling interval	30 s		Real time streams (1 s)	RINEX (1 s)
Elevation cut off	3°		3°	3°
Orbits and ERP	Final IGS products	igswwwwD.sp3 igswwww7.erp	Broadcast + IGS03 correction	Rapid (CODE) CODEwwwwD.EPH CODEwwwwD.ERP
Clock correction	Final IGS products	igswwwwD.sp3	IGS03 stream correction	Rapid (CODE) CODEwwwwD.CLK
A-priori troposphere modeling and mapping funtion	Pre-processing	GMF Boehm et al. (2006b) and VMF Boehm et al. (2006a)	Saastamoinen (1973) dT/cos(z)	GMF Boehm et al. (2006b)
	Parameter estimation	VMF + gridded VMF1 coefficients (00, 06 12 and 18 UTC)	Saastamoinen (1973) dT/cos(z)	VMF + gridded VMF1 coefficients (00, 06 12 and 18 UTC)
	Estimation of horizontal gradients	CHENHER model Chen and Herring (1997) (24 h)	No	No
	Parameter spacing	1 or 2 h	Same as observation	1 h

Table 3 Rejected ZTD estimates ($\sigma_{ZTD} > 0.02$ m)

AC	Data rejected (%)
CHL	7
DGF	0.09
ECU	0.10
IBG	0.06
IGA	23
LUZ	22
UNA	0.06
URY	2

internal consistency and generate the final combined ZTD products (ZTD_{SIR}).

The ZTD_i variance is used as a filter ($\sigma_{ZTD} > 0.02$ m), prior to the combination. The 5% of the ZTD_i values are rejected in the analysed period. Table 3 shows the number of rejected estimates (in %) for each AC.

2.2 ZTD_{SIR} Internal Consistency

Aweighted least-squares combination scheme using the inverse of the input data variances (σ_{ZTD}) as a weighting factor is implemented to estimate ZTD_{SIR} products. Figure 2 shows a detail per year of the number of stations in which the ZTD_i data (3 or more solutions available, with $\sigma_{ZTD} < 0.02$ m) are combined (Nc) compared to the number of stations that had only one solution. For the years 2015–2018 it was possible to have a data redundancy in more than 75% of the stations.

The internal consistency of the ZTD_{SIR} values is evaluated considering the residuals of each contributing ZTD solutions with respect to the combined ZTD value (ZTD_i-ZTD_{SIR}). After a weighted least squares combination process, rms of each ZTD_{SIR} parameters are determined. A mean rms is calculated per station and per year (Table 4). The mean rms

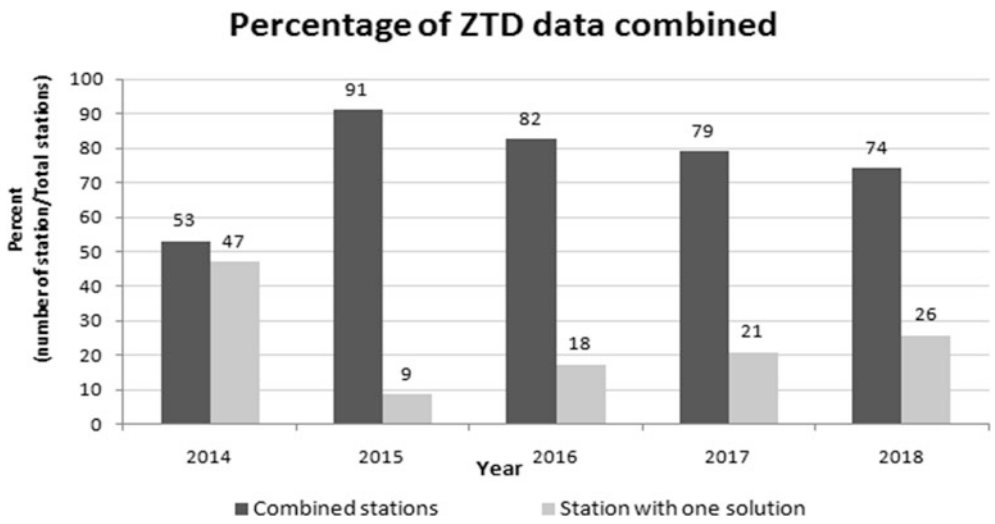

Fig. 2 Number of stations in which ZTD_i data were combined vs stations with one solution

Table 4 Summary of combination process statistics

Year	Nc/Total	%	Mean rms [mm]
2014	180/339	53	0.15
2015	345/378	91	0.09
2016	320/388	82	0.27
2017	308/390	79	0.43
2018	303/409	74	0.54

is less than 1 mm in more than the 84% of the estimated values in the period 2014–2018 (Fig. 3).

2.3 ZTD_{SIR} Validation with IGS Tropospheric Products

For validation, the ZTD final products (ZTD_{SIR}) are compared with the operational IGS (Byram et al. 2011; Byun and Bar-Sever 2009) products (ZTD_{IGS}) at 15 GNSS stations. Figure 4 shows both ZTD time series in two selected stations, AREQ (16.46 °S; 71.49 °W; 2488.92 m.) and OHI2 (63.32 °S; 57.90 °W; 32.47 m.) in the study period (Jan 2014–Dec 2018).

2.4 ZTD_{SIR} Validation with Radiosonde Data

ZTD_{SIR} also, are compared with ZTD values calculated from data of 10 radiosonde stations (ZTD_{RS}). Table 5 details characteristics of the RS used.

The ZTD_{RS} are calculated from the precipitable water for entire sounding (IWV_{RS}), data extracted from radiosonde profiles available at Wyoming Weather Web-University of Wyoming (http://weather.uwyo.edu/upperair/sounding.html). First, ZWD_{RS} values were calculated by Askne and Nordius (1987) with the physical constants for atmospheric refractivity from Rüeger (2002) (Eq. 1). The mean temperature of the atmosphere (Tm) used in (1) is calculated integrating the radiosonde profiles data (temperature and dew-point) in each level profiles up to GNSS station height (Eq. 2). The zenith hydrostatic delay values at the RS sites (ZHD_{RS}) are obtained according to Davis et al. (1985) (Eq. 3), where pressure is calculated to the GNSS height (P_{GNSS}) from pressure radiosonde data. An adaptation to the standard pressure model of Berg (1948) to correct for the height differences is applied (Eq. 4). Finally, ZTD_{RS} values are calculated by adding ZHD_{RS} to ZWD_{RS}

$$ZWD = \frac{\left(22,9744 + \frac{375463}{Tm}\right) 0,4614991785}{10^5} IWV \quad (1)$$

$$Tm = \frac{\int_H^\infty e/T \, dz}{\int_H^\infty e/T^2 \, dz} \quad (2)$$

$$ZHD = 0,002276738. \frac{P_{GNSS}}{1 - 0,00266. \cos(2\varphi) - 0,28.10^{-6}.h_{GNSS}} \quad (3)$$

$$P_{GNSS} = P_{RS}(1 - 0.0000226\ (h_{GNSS} - h_{RS}))^{5.225} \quad (4)$$

2.5 ZTD Estimation Applying PPP

In order to have a product in near real time to be used in numerical weather prediction model, we tested the Precise

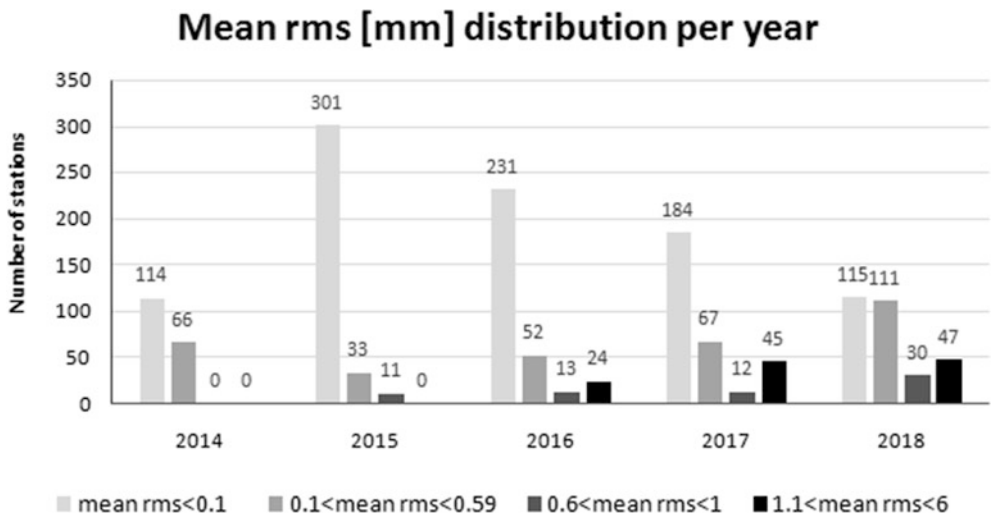

Fig. 3 Distribution of the ZTD_{SIR} mean rms per year (2014–2018)

Point Positioning processing technique (ZTD_{PPP}). Two case of study are analysed

- Case 1: Feb 21 to Mar 27 (36 days), 2016; ten GNSS stations (located in the central-western region of South America).
- Case 2: Jan 1 to Dec. 31, 2019 (365 days); thirty GNSS stations (located in Argentina).

The ZTD_{PPP} values estimated are compared with the corresponding ZTD_{SIR} values.

This estimation approached with two softwares, BNC (Weber et al. 2016) and BSW52, in the first case study. PPP with BSW52 showed better results (not shown). In the second period (year 2019) we decided to estimate ZTD_{PPP} only by BSW52. In both cases of study, with BSW52 PPP, rapid IGS products (orbits, ERP and satellite clock corrections) were used so the ZTD_{PPP} were estimated with 24 h delay. Table 2 summarizes the input data, models and main configuration used for each software.

2.6 Determination of IWV Values from GNSS-Based ZTD Estimates

The GNSS-based ZTD values are used to calculate the IWV applying the ratio of Askne and Nordius (1987) to the wet component of the delay (ZWD), (Eq. 1). In this work, the ZTD_{SIR} and the one from applying PPP (from BSW52) were used. ZWD values were obtained by removing the ZHD, which was calculated according to Davis et al. (1985) (Eq. 3). Sea level pressure values (P_{ref}) were extracted from the ERA-Interim products and were reduced to the height of the GNSS stations (P_{GNSS}) following Berg (1948) (Eq. 5).

$$P_{GNSS} = P_{ref}.\left(1 - 0,0000226.\left(h_{GNSS} - h_{ref}\right)\right)^{5,225} \quad (5)$$

In this case, the weighted mean temperature of the atmosphere (Tm) was calculated in accordance with Mendes (1999) using the surface temperature (Ts) also provided by ERA-Interim. The values for the refractivity constants were taken from Rüeger (2002). Following this strategy, IWV_{SIR} series from a 5 years (2014–2018) period were estimated in each SIRGAS station. We generated four daily IWV maps by Hunter (2007) (at 00:00, 06:00, 12:00 and 18:00 UTC) for the entire SIRGAS region, see some examples in Fig. 5 (24-6-2018).

The IWV_{SIR} values were tested in the 10 radiosonde stations selected (Table 5). The Figs. 6 and 7 show the comparison of IWV_{SIR} (inferred from ZTD_{SIR}) values with values obtained from radiosonde profiles (IWV_{RS}) at two SIRGAS stations: MZAC (located in an arid region) and IGM1 (located in a humid region), respectively.

3 Results

3.1 ZTD_{SIR} Validation

Our results presented a quite good agreement with the IGS products (see Fig. 4). Discrepancies between ZTD_{SIR} and ZTD_{IGS} values are compared at 15 IGS (SIRGAS) stations (Fig. 8). The results present a mean root mean square (rms) value of 6.8 mm (0.29% of the mean ZTD) with a negative mean bias of 1.5 mm (0.07% of the mean ZTD).

The comparison of ZTD_{SIR} w.r.t. ZTD_{RS} is also very promising: discrepancies computed at 10 radiosonde stations (see Fig. 1 and Table 5) have a mean rms of 7.5 mm (0.32% of the mean ZTD) and a negative mean bias of 2 mm (0.09%

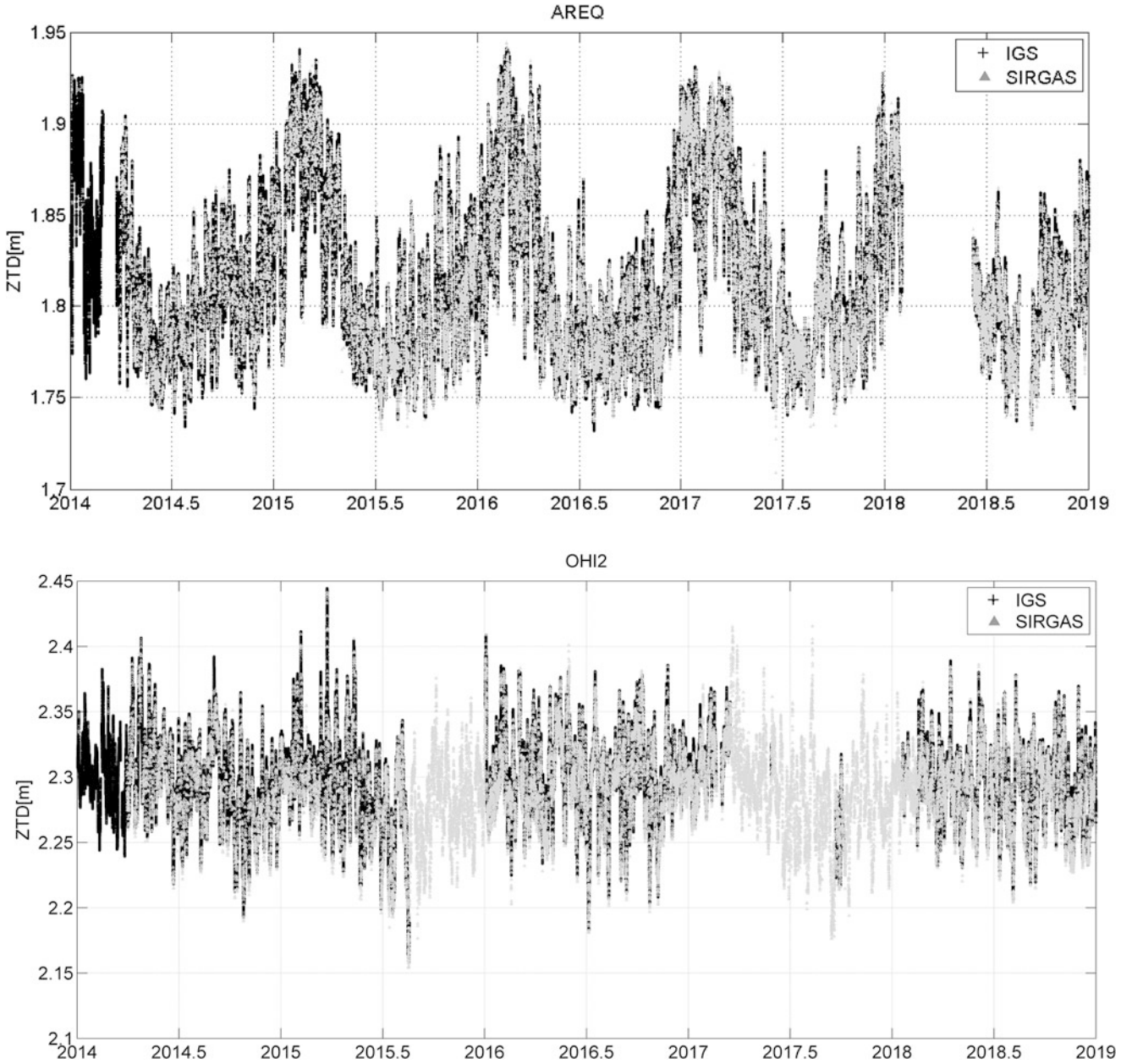

Fig. 4 Time series of ZTD_{SIR} (grey) and ZTD_{IGS} (black) values at two selected SIRGAS stations, AREQ (Arequipa, Peru) and OHI2 (O'Higgins, Antartica), period: Jan 2014–Dec 2018

Table 5 Location of ten RS stations used (bold used in ZTD_{PPP} validation), distance to GNSS sites, and heights (h_{GNSS} and h_{RS})

RS station	GNSS site	Lat. (°)	Long. (°)	h_{RS} (m)	h_{GNSS} (m)	Distance (km)
78866 (TNCM)	SMRT	18.03	−63.09	9	−32.48	3
78897 (TFFR)	ABMF	16.21	−61.41	8	−25.57	12
78807 (MPCZ)	IGN1	8.98	−79.46	19	47.56	13
82280	SALU	−2.53	−44.28	51	18.99	11
82397	CEFT	−3.59	−38.45	19	4.90	15
87155 (SARE)	**CHAC**	**−27.36**	**−59.04**	**52**	**77.95**	**10**
87418 (SAME)	**MZAC**	**−32.83**	**−68.78**	**704**	**859.86**	**13**
87623 (SAZR)	**SRLP**	**−36.57**	**−64.27**	**191**	**223.83**	**7**
87344 (SACO)	**CORD**	**−31.32**	**−64.22**	**474**	**746.83**	**34**
87576 (SAEZ)	**IGM1**	**−34.65**	**−58.42**	**20**	**50.69**	**28**

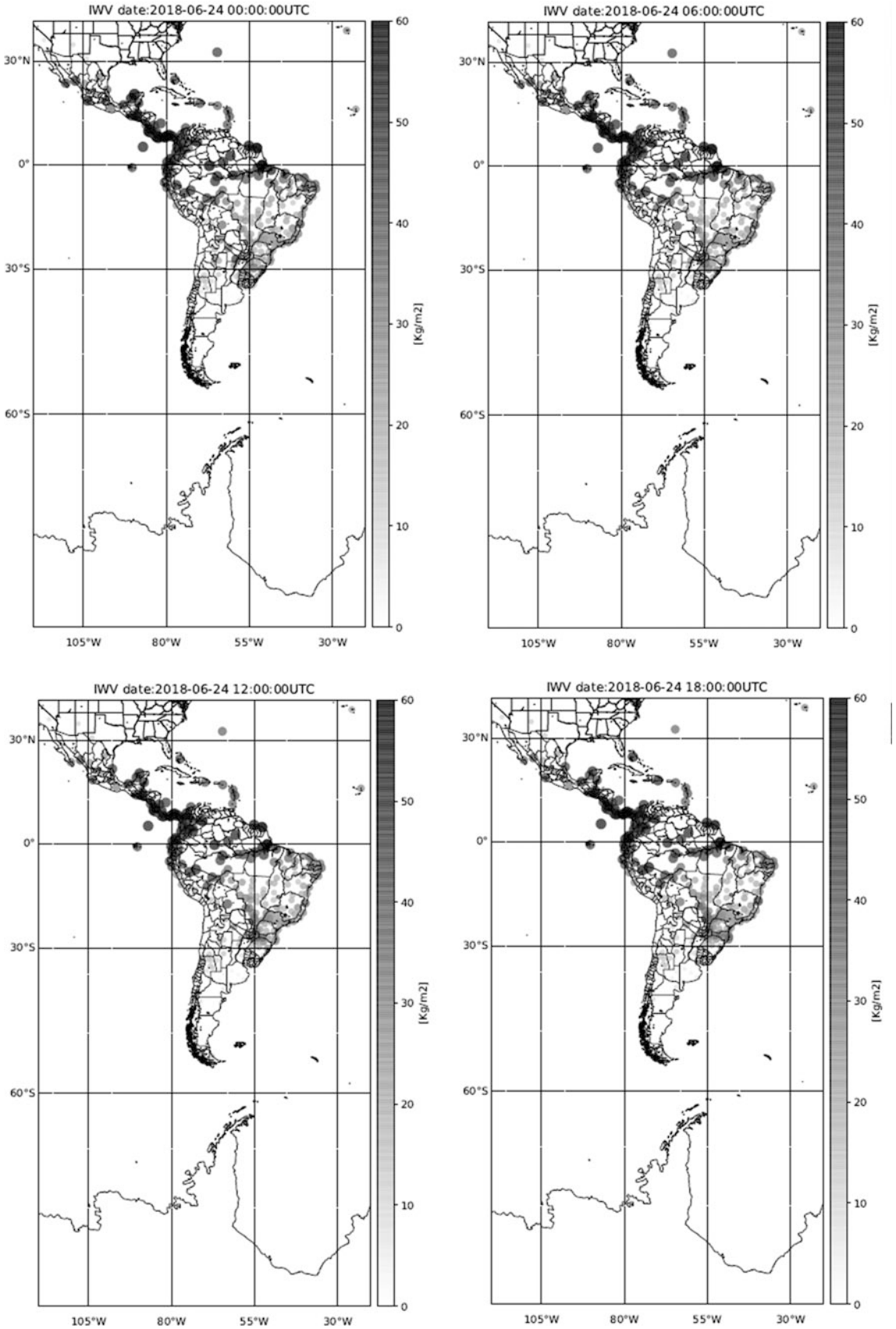

Fig. 5 Maps of IWV inferred from the ZTD estimates produced within the operational SIRGAS processing (24-6-2018; 00,06,12 and 18 hs UTC)

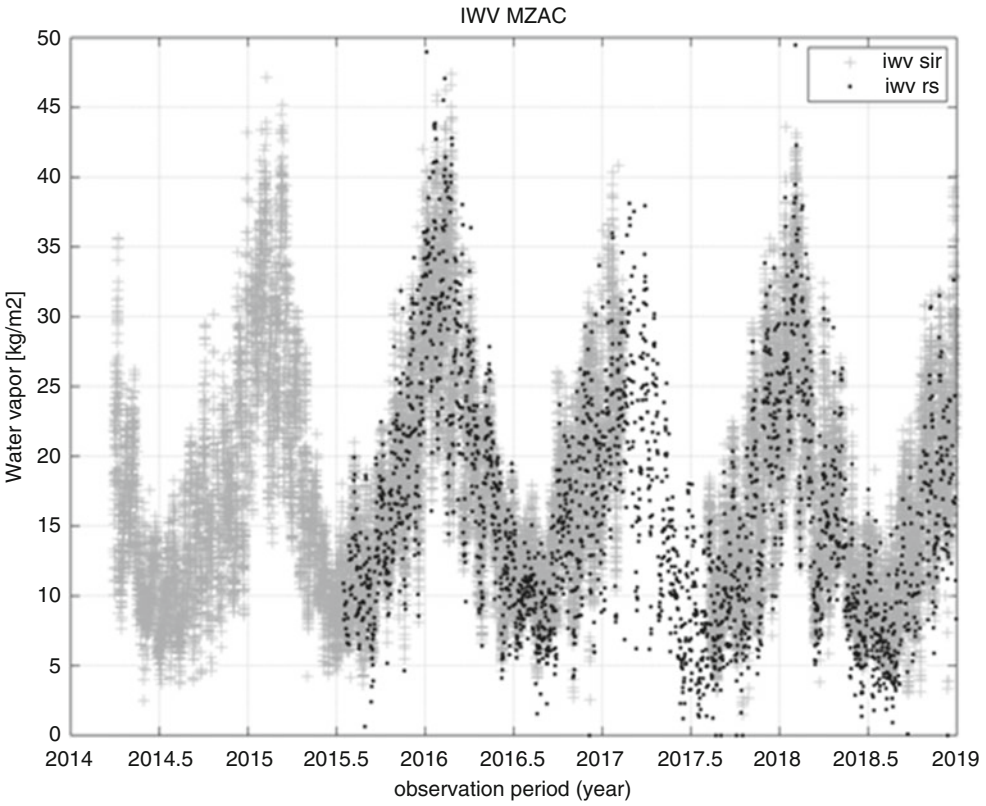

Fig. 6 IWV_{SIR} (MZAC GNSS station) and IWV_{RS} (RS: SAME)

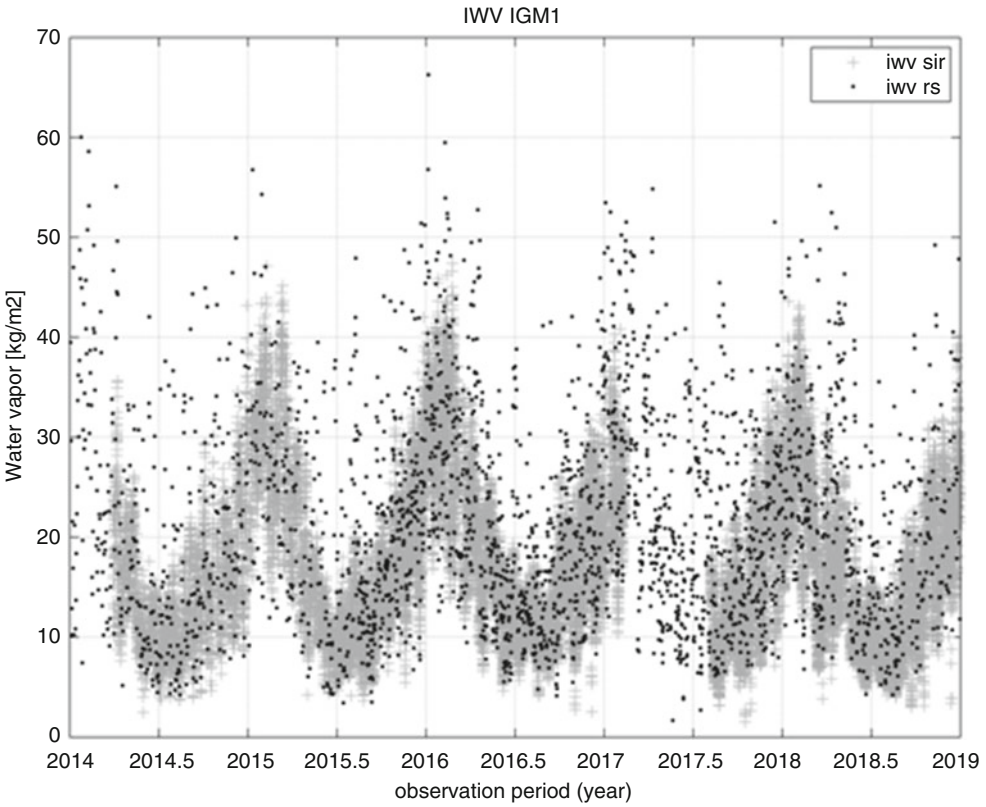

Fig. 7 IWV_{SIR} (IGM1 GNSS station) and IWV_{RS} (RS: SAEZ)

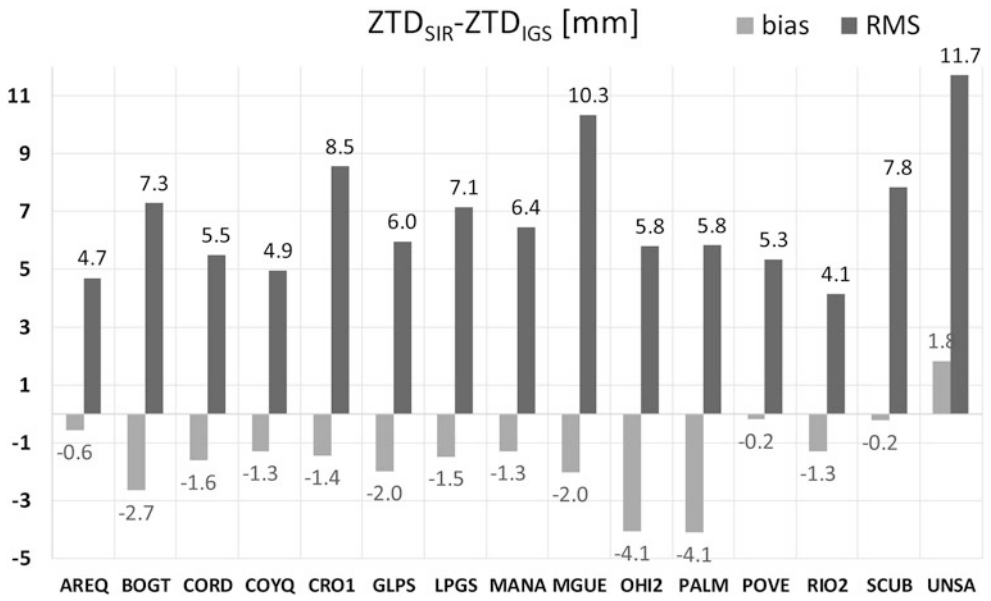

Fig. 8 Comparison of ZTD_{SIR} and ZTD_{IGS} values at 15 selected SIRGAS stations (Jan 2014–Dec 2018)

of the mean ZTD). An analysis of the radiosonde types has been started at each analysed site, which it could be the cause for the negative bias in line with the results of Wang et al. (2007) and Pacione et al. (2017).

3.2 ZTD_{PPP} Products Validation

Analysing the ZTD_{PPP} products, the BSW52-based ZTD_{PPP} estimates showed a better agreement than the BNC-based ZTD_{PPP} estimates with respect to the corresponding ZTD_{SIR} values. The rms and bias are the two indexes for the evaluation of the two estimations. Results of these two-test data set are shown in Table 6. BNC-based ZTD_{PPP} estimates were less accurate as expected because real time IGS product were used. It may also be a consequence of the fact that ZTD_{SIR} and the BSW52-based ZTD_{PPP} use the same models to determine the tropospheric parameters. In the case 2 a bias-reduction scheme was implemented on a monthly basis as applied in Douša and Vaclavovic (2014).

The comparison of the BSW52-based ZTD_{PPP} estimates and ZTD_{SIR} values at two selected SIRGAS station, EBYP (in a subtropical region) and MGUE (in an arid region), with the data in the case 1, are shown in Fig. 9.

The discrepancies between the ZTD_{PPP} values estimated in the second case of study (Year 2019, 30 stations) with the respectively ZTD_{SIR} values were also very promising (Fig. 10). The mean rms and mean bias per station is shown in the Fig. 10. The 84% of the stations had a mean rms < 28 mm and the rest 16% had a mean rms < 31 mm.

Table 6 Comparison of ZTD_{PPP} values with the operational SIRGAS processing (ZTD_{SIR})

Case	Software	Bias [mm]	rms [mm]
Case 1 2016 (36 days), 10 GNSS stations	BSW52	49 (1.8% of the ZTD)	55
	BNC	118 (4.8% of the ZTD)	125
Case 2 2019 (365 days), 30 GNSS stations	BSW52	2 (0.07% of the ZTD)	22

In five GNSS stations, the BSW52-based ZTD_{PPP} estimates were validated with respect to ZTD_{RS} (detailed in bold in Table 5). Figure 11 shows this comparison in the IGS (SIRGAS) station CORD in the centre of Argentina, as an example.

3.3 IWV_{SIR} Validation

The IWV_{SIR} validation with IWV_{RS} also showed agreement. The results for a period of 5 years, in 10 RS – GNSS locations yielded a mean bias 0.41 kg/m^2 and a mean rms 3.5 kg/m^2. The correlation coefficient of the two series (IWV_{SIR} and IWV_{RS}) presented in Fig. 12 is 0.94, which indicates a very good agreement between both estimations.

In the other hand, the comparison of IWV_{PPP} (calculated from the BWS52-based ZTD_{PPP} values) with IWV_{RS}, produces discrepancies with a mean rms of 1 kg/m^2, a standard deviation of 0.73 kg/m^2 and a bias of 2.37 kg/m^2 (not shown).

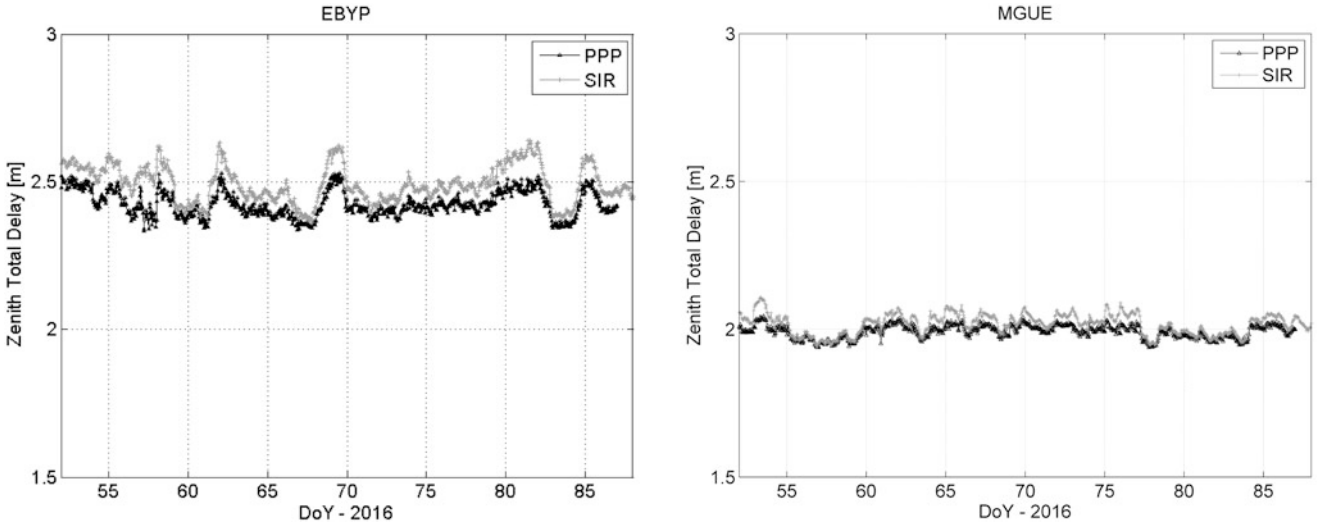

Fig. 9 Comparison of ZTD_{SIR} and BSW52-based ZTD_{PPP} values at two selected SIRGAS stations

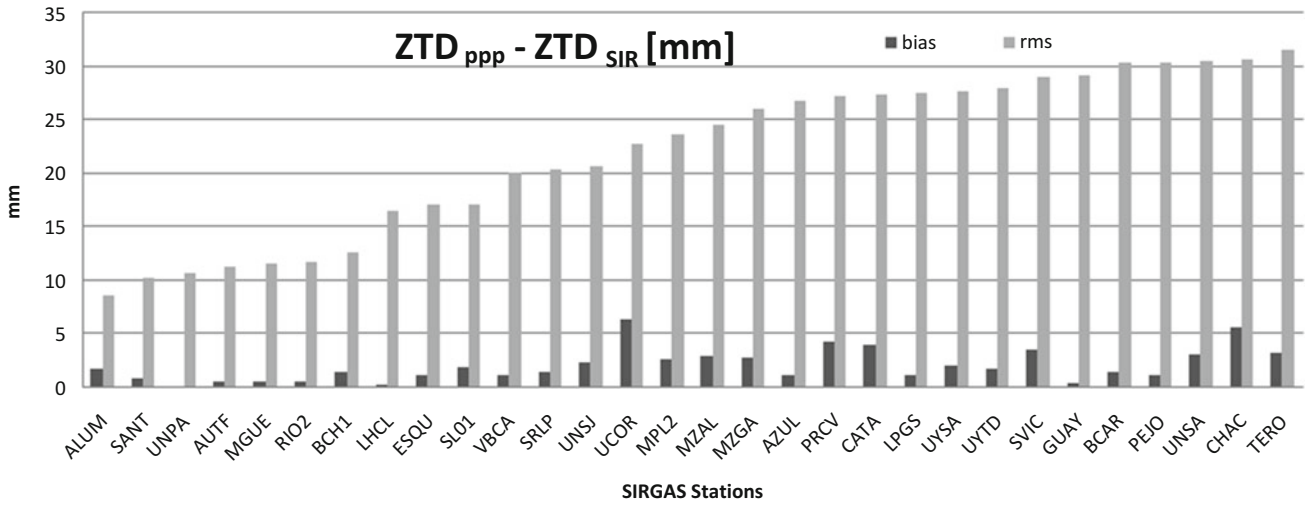

Fig. 10 Comparison of BWS52-based ZTD_{PPP} with ZTD_{SIR} at 30 GNSS station (365 days)

4 Conclusions

Latin America has SIRGAS network, an infrastructure of GNSS stations that generates ZTD (per hour), offering regional and continental coverage that can be used in atmospheric studies.

The internal consistency of the ZTD_{SIR} values, calculated by SIRGAS ACs, have been evaluated for a period of 5 years (2014–2018). An average rms less than 1 mm, in more than the 84% of the values, indicate the rigorous weighted least squares combination process implemented to get the SIRGAS reference products.

The ZTD_{SIR} series for a 5-year period have been validated with two different time series. They agree with the corresponding values of the ZTD series obtained by the IGS (mean rms 6.8 mm; mean bias −1.5 mm) as well as those from the radiosonde technique (mean rms 7.5 mm; mean bias −2 mm).

The ZTD obtained by PPP with BSW52, using the RAPID CODE products (ephemeris and clock corrections) are validated with respect to the post-processing products ZTD_{SIR}. The mean rms of the differences is 22 mm (84% of the stations had a mean rms < 28 mm) for an annual case of study (2019, 30 stations). It remains to continue improving the methodology to increase accuracy and decrease the positive bias that on average resulted in 2 mm (0.07% of the ZTD mean value in the stations evaluated). Anyway, these accuracy of ZTD_{PPP} complies with the threshold requirements for the operational NWP nowcasting – the relative accuracy of 5 kg/m^2 in integrated water vapor (IWV) and 30 mm in ZTD when approximating the conversion factor defined by Bevis

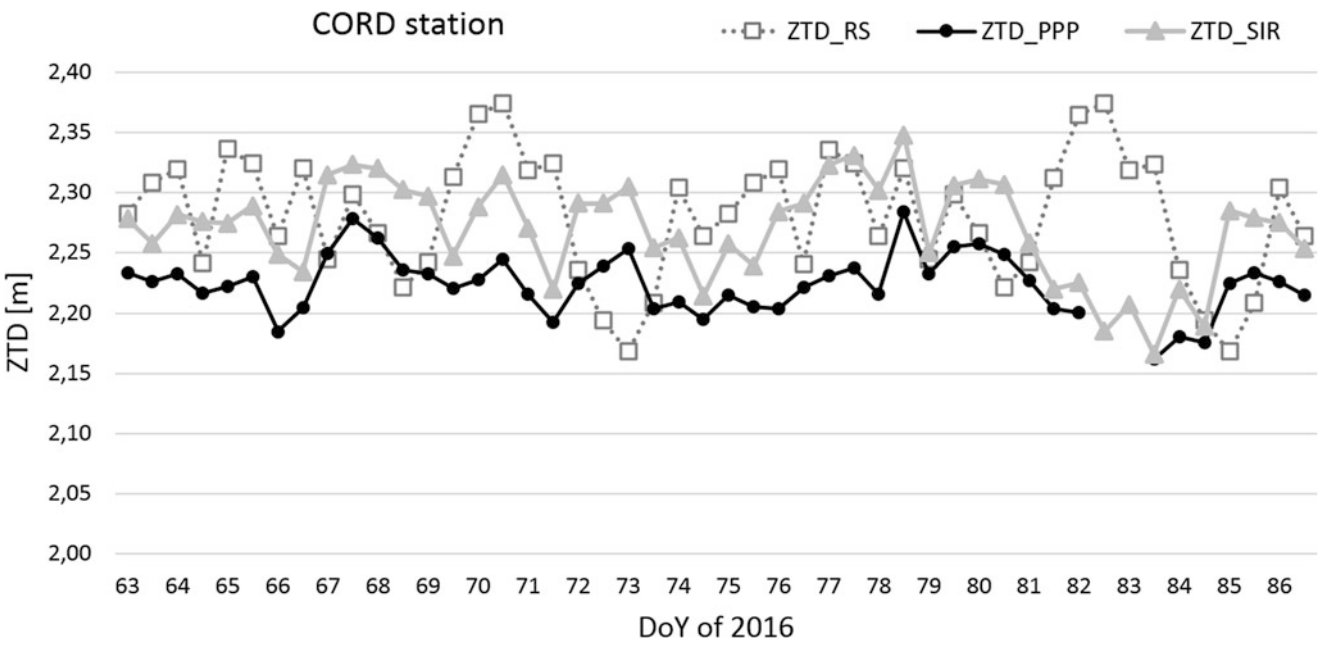

Fig. 11 Time series of ZTD_{SIR}, BWS52-based ZTD_{PPP} and ZTD_{RS} values at a GNSS station located in Cordoba (Argentina)

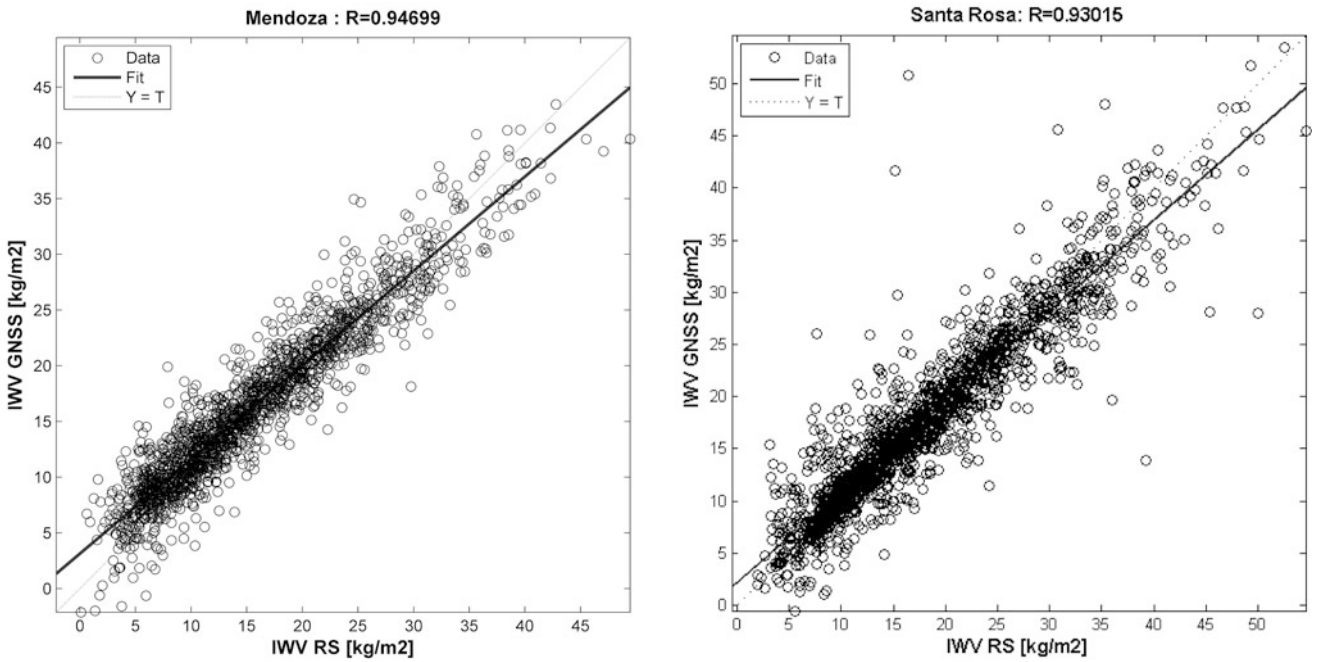

Fig. 12 Scatter plot comparing IWV values inferred from GNSS-based ZTD estimates (IWV_{SIR}) and radiosonde profile data (IWV_{RS}) at two selected SIRGAS stations (Jan 2014 to Dec 2018)

et al. (1994) and Douša and Vaclavovic (2014). However, we must work to obtain a product in near real time (with 90 min of latency), applying ultra-rapid orbits and clocks, or even better using real-time corrections (Guerova et al. 2016).

The publication of this new product from SIRGAS opens the opportunity for new research topics that can be carried out both continentally and regionally in Latin America. As an example, it has been shown that SIRGAS ZTD products can be used to calculate the IWV over SIRGAS stations, thus providing IWV with a spatial and temporal density not existing in Latin America by conventional techniques. This variable has also been validated with radiosonde data (mean correlation coefficient 0.89, in 10 compared sites). SIRGAS ZTD products can be used as a reference for

different scientific applications (e.g. validation of regional numerical weather prediction reanalyses) and they could be used for monitoring trends and variability in atmospheric water vapour in Latin America region, similar than EUREF Permanent network (Pacione et al. 2017).

Acknowledgments The authors are grateful for the silent task of those responsible for the GNSS stations, the data centers and the SIRGAS analysis centers (CHL, DGF, ECU, IBG, IGA, LUZ, URY and UNA), without which this research could not have been carried out.

The ERA-Interim data used were provided by ECMWF. Radiosonde data were provided by Wyoming Weather Web, University of Wyoming.

References

Askne J, Nordius H (1987) Estimation of tropospheric delay for microwaves from surface weather data. Radio Sci 22:379–386. https://doi.org/10.1029/RS022i003p00379

Berg H (1948) Allgemeine Meteorologie. Dümmler's Verlag, Bonn, p 337

Bevis M, Businger S, Chiswell S, Herring TA, Anthes RA, Rocken C, Ware RH (1994) GPS meteorology: mapping zenith wet delays onto precipitable water. J Appl Meteorol 33:379–386

Bianchi CE, Mendoza LPO, Fernández LI, Natali MP, Meza AM, Moirano JF (2016) Multi-year GNSS monitoring of atmospheric IWV over central and South America for climate studies. Ann Geophys 34:623–639

Boehm J, Niell AE, Tregoning P, Schuh H (2006a) Global mapping function (GMF): a new empirical mapping function based on numerical weather model data. Geophys Res Lett 33:25. https://doi.org/10.1029/2005GL025546

Boehm J, Werl B, Schuh H (2006b) Troposphere mapping functions for GPS and very long baseline interferometry from European Centre for Medium-Range Weather Forecasts operational analysis data. J Geophys Res 111:B02406. https://doi.org/10.1029/2005JB003629

Bonafoni S, Mazzoni A, Cimini D, Montoponi M, Pierdicca N, Basili P, Ciotti P, Carlesimo G (2013) Assessment of water vapor retrievals from a GPS receiver network. GPS Solut 17(4):475–484

Brunini C, Sánchez L, Drewes H, Costa S, Mackern V, Martínez W, Seemuller W, da Silva A (2012) Improved analysis strategy and accessibility of the SIRGAS reference frame. In: Kenyon S, Pacino M, Marti U (eds) Geodesy for planet earth. International association of geodesy symposia, vol 136. Springer, Berlin, pp 3–10

Bruyninx C, Legrand J, Fabian A et al (2019) GNSS metadata and data validation in the EUREF permanent network. GPS Solut 23:106. https://doi.org/10.1007/s10291-019-0880-9

Byram S, Hackman C, Tracey J (2011) Computation of a high-precision GPS-based troposphere product by the USNO. In: Proceedings of the 24th international technical meeting of the satellite division of the institute of navigation (ION GNSS 2011). 2001

Byun SH, Bar-Sever YE (2009) A new type of troposphere zenith path delay product of the international GNSS service. J Geod 83(3–4):1–7

Calori A, Santos JR, Blanco M, Pessano H, Llamedo P, Alexander P, de la Torre A (2016) Ground-based GNSS network and integrated water vapor mapping during the development of severe storms at the Cuyo region (Argentina). Atmos Res 176–177:267–275

Camisay MF, Rivera JA, Mateo ML, Morichetti PV, Mackern MV (2020) Estimation of integrated water vapor derived from global navigation satellite system observations over Central-Western Argentina (2015–2018). Validation and usefulness for the understanding of regional precipitation events. J Atmos Sol Terr Phys 197:105143. https://doi.org/10.1016/j.jastp.2019.105143. ISSN 1364-6826

Chen G, Herring TA (1997) Effects of atmospheric azimuthal asymmetry on the analysis of space geodetic data. J Geophys Res 102:20,489–20,502

Cioce V, Martínez W, Mackern MV, Pérez R, De Freitas S (2018) SIRGAS: reference frame in Latin America. Coordinates XIV(6):6–10. ISSN 0973-2136

Dach R, Lutz S, Walser P, Fridez P (2015) Bernese GNSS software version 5.2. Astronomical Institute, University of Bern, Bern. https://doi.org/10.7892/boris.72297. ISBN: 978-3-906813-05-9; Open Publishing

Davis JL, Herring TA, Shapiro I, Rogers AE, Elgened G (1985) Geodesy by interferometry: effects of atmospheric modeling errors on estimates of base line length. Radio Sci 20:1593–1607

Douša J, Vaclavovic P (2014) Real-time zenith tropospheric delays in support of numerical weather prediction applications. Adv Space Res 53:1347–1358. https://doi.org/10.1016/j.asr.2014.02.021

Fernández LI, Salio P, Natali MP, Meza AM (2010) Estimation of precipitable water vapour from GPS measurements in Argentina: validation and qualitative analysis of results. Adv Space Res 46:879–894

Guerova G, Jones J, Douša J, Dick G, de Haan S, Pottiaux E, Bock O, Pacione R, Elgered G, Vedel H, Bender M (2016) Review of the state of the art and future prospects of the ground-based GNSS meteorology in Europe. Atmos Meas Tech 9:5385–5406. https://doi.org/10.5194/amt-9-5385-2016

Hunter JD (2007) Matplotlib: a 2D graphics environment. Comp Sci Eng 9(3):90–95

Llamedo P, Hierro R, de la Torre A, Alexander P (2017) ENSO-related moisture and temperature anomalies over South America derived from GPS radio occultation profiles. Int J Climatol 37:268–275

Mendes VB (1999) Modeling the neutral-atmosphere propagation delay in radiometric space techniques. Ph.D. dissertation, Department of Geodesy and Geomatics Engineering Technical Report No 199, Univ. of New Brunswick, Canada

Pacione R, Araszkiewicz A, Brockmann E, Dousa J (2017) EPN-Repro2: a reference GNSS tropospheric data set over Europe. Atmos Meas Tech 10:1689–1705. https://doi.org/10.5194/amt-10-1689-2017

Rüeger JM (2002) Refractive index formula for radio waves. In: Proc. XXII FIG Int. Congr., April 19–26, 2002, Web. http://www.fig.net/resources/proceedings/fig_proceedings/fig_2002/Js28/JS28_rueger.pdf

Saastamoinen J (1973) Contributions to the theory of atmospheric refraction. Bull Geod 107:13–34. https://doi.org/10.1007/BF02521844

Sánchez L, Drewes H, Brunini C, Mackern MV, Martínez-Díaz W (2015) SIRGAS core network stability. In: Rizos C, Willis P (eds) IAG 150 years. International Association of Geodesy Symposia, vol 143. Springer, Cham, pp 183–191

Van Baelen J, Aubagnac JP, Dabas A (2005) Comparison of near–real time estimates of integrated water vapor derived with GPS, Radiosondes, and microwave radiometer. J Atmos Ocean Technol 22:201–210

Wang J, Zhang L, Dai A, Van Hove T, Van Baelen J (2007) A near-global, 2-hourly data set of atmospheric precipitable water dataset from ground-based GPS measurements. J Geophys Res 112:D11107. https://doi.org/10.1029/2006JD007529

Weber G, Mervart L, Stürze A, Rülke A, Stöcker D (2016) BKG Ntrip Client, Version 2.12. Mitteilungen des Bundesamtes für Kartographie und Geodäsie, vol 49. Frankfurt am Main, 2016